Tracking Merged Objects within Non-Resolved Imagery

Calum Meredith
Defence Science and Technology Laboratory, UK
Paul Chote, Robert Airey
University of Warwick, UK

ABSTRACT

The PHANOM ECHOES 2 experiment studied the rendezvous and proximity operations of Intelsat 10-02 and Mission Extension Vehicle 2 (MEV2), which provided an opportunity to collect telescope imagery of the two satellites while they were closely-spaced. Different telescopes were used during the study, including the University of Warwick's Test Complementary Metal Oxide Semiconductor (CMOS) Telescope, and this allowed the satellites to be individually resolved at a range of different angular separations. Where this was not possible the two satellites appeared merged into a single point spread function. We show how modelling of the point spread functions of the two satellites, particularly during observed 'glint' events, can be used to retrieve the angular separation of the two satellites even when they are not individually resolvable. The technique is compared with data from the Liverpool Telescope, used as ground-truth, and a parameter sensitivity analysis is undertaken to determine its accuracy.

1. INTRODUCTION

Maintaining tracks on geostationary orbiting (GEO) spacecraft and other closely-spaced objects when they are in close proximity has key importance within Space Domain Awareness (SDA) for understanding satellite cluster behaviour, conjunction events and the intentions of nearby manoeuvring satellites. When two satellites carry out rendezvous and proximity operations, or similar activities, the ability to separate and distinguish between the two objects using electro-optical techniques can be challenging: at a particularly close angular separations, the two objects appear merged within an image and become unable to be individually resolved.

However, if one object displays glinting behaviour (for example, whilst manoeuvring), it is possible to constrain the relative position and separation of each object by modelling the small fractional shift in the centroid of the unresolved point-spread function. An investigation of this technique has been performed by Dstl and the University of Warwick using data which was obtained from the Warwick Test CMOS test telescope during PHANTOM ECHOES 2.

2. OBSERVATION CAMPAIGN

Between February and April 2021, the MEV-2 conducted rendezvous and docking with Intelsat 10-02, and was the subject of a coordinated experiment, known as PHANTOM ECHOES 2, exploring options to improve allied capabilities for protection of spacecraft in GEO. PHANTOM ECHOES 2 was previously reported at AMOS 2021 and 2022 [1, 2].

The PHANTOM ECHOES 2 experiment involved defence science and technology (S&T) agencies of the Five-Eyes (FVEY) nations – Australia, Canada, New Zealand, the United Kingdom and the United States, – to exploit this opportunity to successfully pursue a coordinated SDA experiment, observing and scrutinising the dynamics and behaviours of the two satellites using a variety of ground- and space-based sensors.

Two sensors involved in this experiment were the Warwick Test CMOS test telescope and the Liverpool Telescope. Both of these telescopes are located on La Palma, Canary Islands, within 200 m of each other. The parameters of these sensors are included in Table 1. The Warwick Test CMOS Telescope was used in this study as a primary source of data with the Liverpool Telescope providing a reference ground truth. The Field of View of the Warwick

Test CMOS Telescope is larger than that of the Liverpool Telescope but has a pixel scale of 4.35 arcsec / pixel compared with Liverpool Telescope's 0.2 arcsec / pixel. This results in higher precision of positional information about sources that can be extracted from the Liverpool Telescope data and, when observation conditions, allow can act a reference groundtruth to lower performance sensors. Residual inaccuracies remain on the order of the pixel scale. Other sources of groundtruth considered, such as satellite telemetry, were either not available or not at an appropriate temporal resolution for utility in this study.

Table 1

Telescope	**Description**	**Aperture**	**FOV**	**Pixel Scale**
Warwick Test CMOS	Newtonian reflector	0.18m	2.48° x 2.48°	4.35 arcsec / pixel
Liverpool Telescope	Cassegrain reflector, Ritchey-Chrétien hyperbolic optics	2m	0.17° x 0.17°	0.2 arcsec / pixel

The two telescopes were utilised throughout the PHANTOM ECHOES 2 experiment to observe the proximity operations of Intelsat 10-02 and MEV2. The Liverpool Telescope has a higher resolving power (as per Table 1) and could resolve the two satellites when they were at closer angular separations than the Warwick Test CMOS telescope. Fig. 1 provides two examples of observations using both the Warwick and the Liverpool telescopes taken 41 seconds apart when both Intelsat 10-02 and MEV2 are within the target field. The much smaller field of view of the Liverpool Telescope is demonstrated as well as its resolving power. In Fig. 2 the same observations of the target satellites are presented at roughly the same angular aspect ratio for the two telescopes. It is demonstrated that the Liverpool Telescope can observe two (overlapping) sources, being the two satellites, while for the Warwick Test CMOS Telescope these are completely merged.

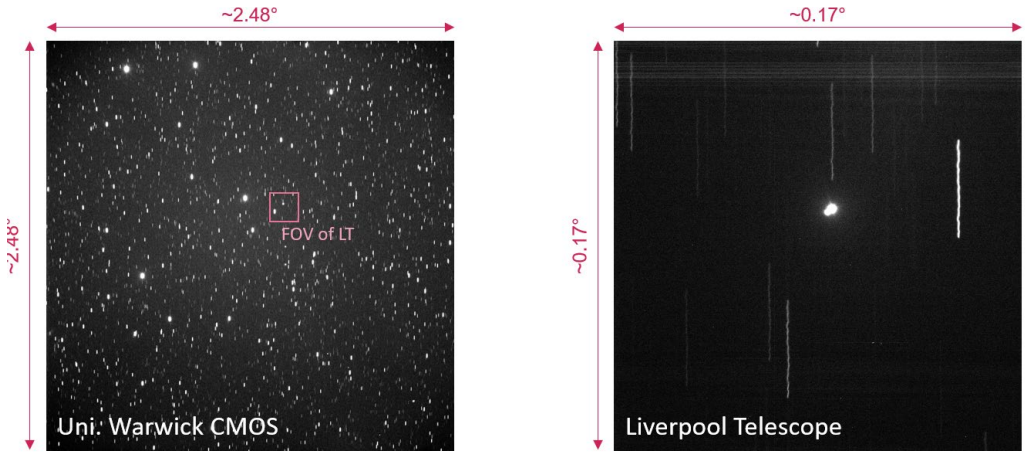

Fig. 1. Observation data from 17 February 2021 ~00:33 UTC from (a) Warwick Test CMOS (b) Liverpool Telescope

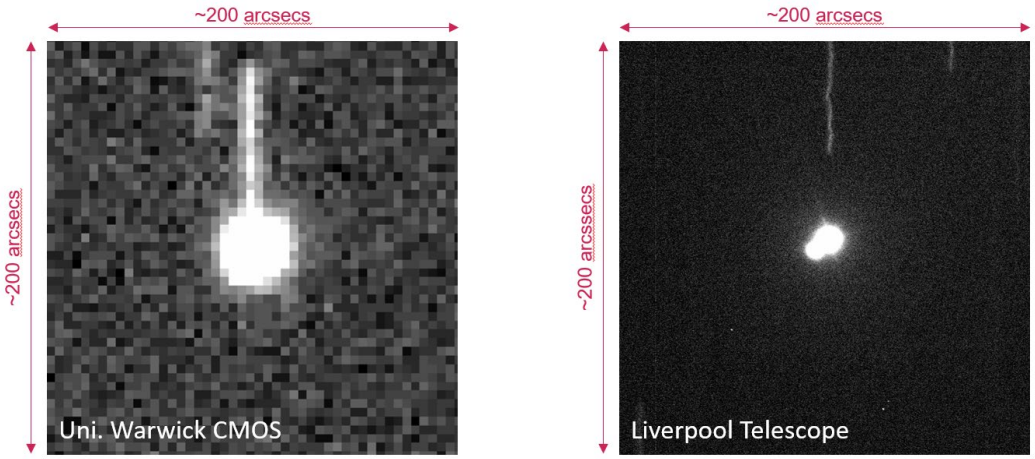

Fig. 2 – The same data as presented in Fig. 1 demonstrating typical characteristics of the Warwick CMOS and the Liverpool Telescope.

Due to the availability of the Liverpool Telescope it was only utilised for a limited number of observation periods during the experiment, whereas the Warwick Test CMOS Telescope was observing regularly throughout the period. The Warwick Test CMOS Telescope was able to observe over full nights and generate light curves of the two satellites. The entire dataset of light curves collected is presented in Fig. 3. The light curves are plotted with solar phase angle, which is the angle between the direction to the sun and the direction to the observer, with respect to the satellite. This is determined from the extracted satellite position information from the data and is a way of identifying features that vary with illumination conditions. Depending on the angular separation of the two satellites at different times, light curves were generated for the three cases of observing Intelsat 10-02 in isolation, MEV2 in isolation and also where they appear merged or blended (as is the case in Fig. 2).

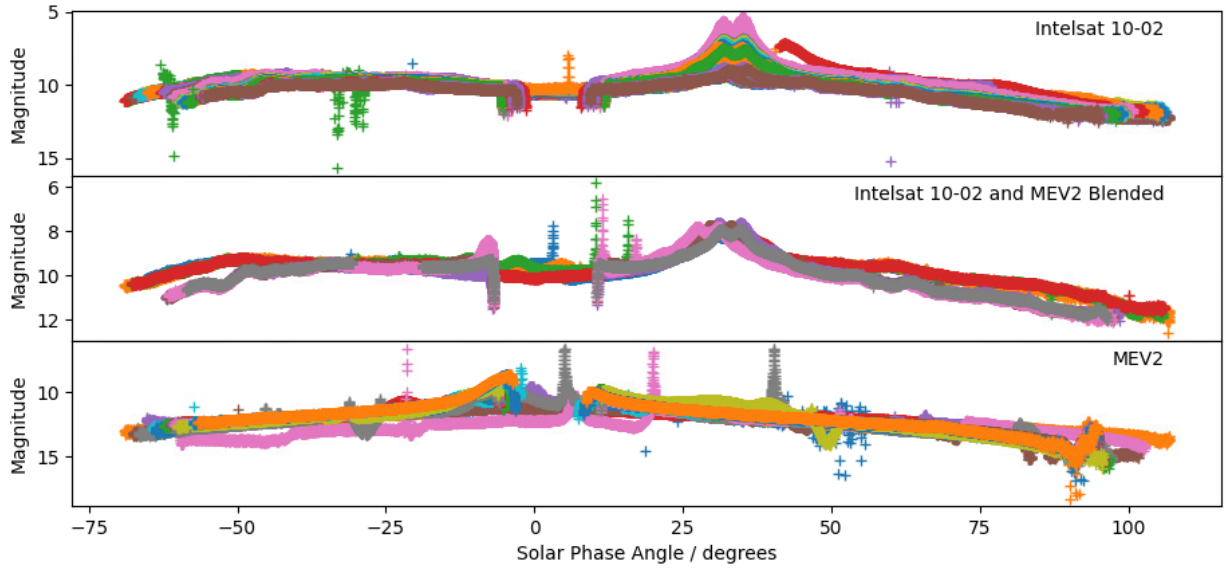

Fig. 3. (top) Light curves obtained by the Warwick Test CMOS Telescope of Intelsat 10-02; (middle) Intelsat 10-02 and MEV2 while non-resolved; (bottom) MEV2.

The process of reduction and analysis of this data, and others, is current in preparation [3]. However, for the purpose of this study, on nights where each object could be individually resolved within the telescope field-of-view, the collected data could be used to understand the bulk signature and brightness magnitude of each satellite. It is noted that Intelsat 10-02 appears to exhibit similar light curve characteristics with solar phase angle for each set of observations.. The light curves of MEV2 are more difficult to interpret but is typically significantly less bright than

MEV2. However, there are notable brief 'glint' conditions when MEV2 is brighter than Intelsat 10-02 (particularly clearly observed in the peaks of the pink and grey light curve observation lines for MEV2 in Fig. 3). This glinting behavior is less apparent for Intelsat 10-02.

When the blended light curve is considered, as expected, its bulk properties are very similar to that of the significantly brighter Intelsat 10-02. However, glinting behavior is also observed (in Fig. 3 at close to 10 degrees phase angle), and this is hypothesized to be where the glinting behavior of MEV2 is significant enough to dominate during these time periods when the data was collected. It is difficult, with current data, to understand the cause of the glint behavior, it is of short duration and could be due to maneuvering of MEV2 presenting different features of the satellite during observations or a feature of the satellite bus that varies with solar phase angle in isolation.

3. OBSERVED GLINTS AND CENTROID DEVIATION

Examples of glinting behavior as observed in the original Warwick Test CMOS telescope data, where Intelsat 10-02 and MEV2 are still separable, is presented in Fig. 4. The data from the telescope has its background subtracted using the Photutils *Background2D* and *MedianFilter* functions [4]. This demonstrates its behavior in that the significant brightness increase of ~2-3 times the peak flux of Intelsat 10-02 occurs for only a short duration ~5 minutes. Fig. 5 similarly presents an occasion when the two satellites appear merged into one point spread function in the observations but a similar glint is observed.

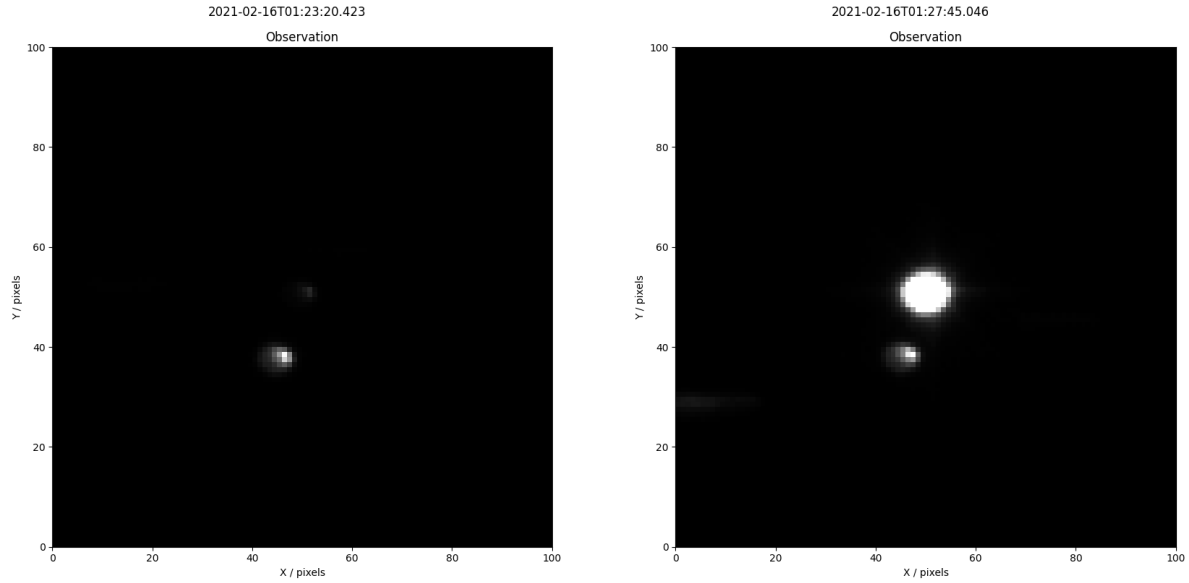

Fig. 4 - Intelsat 10-02 and MEV2 observed using the Warwick Test CMOS Telescope. (left) observations showing Intelsat 10-02 as the source brighter than MEV2. (right) a few minutes later a 'glint' of the MEV2 source is observed showing how it becomes significantly brighter.

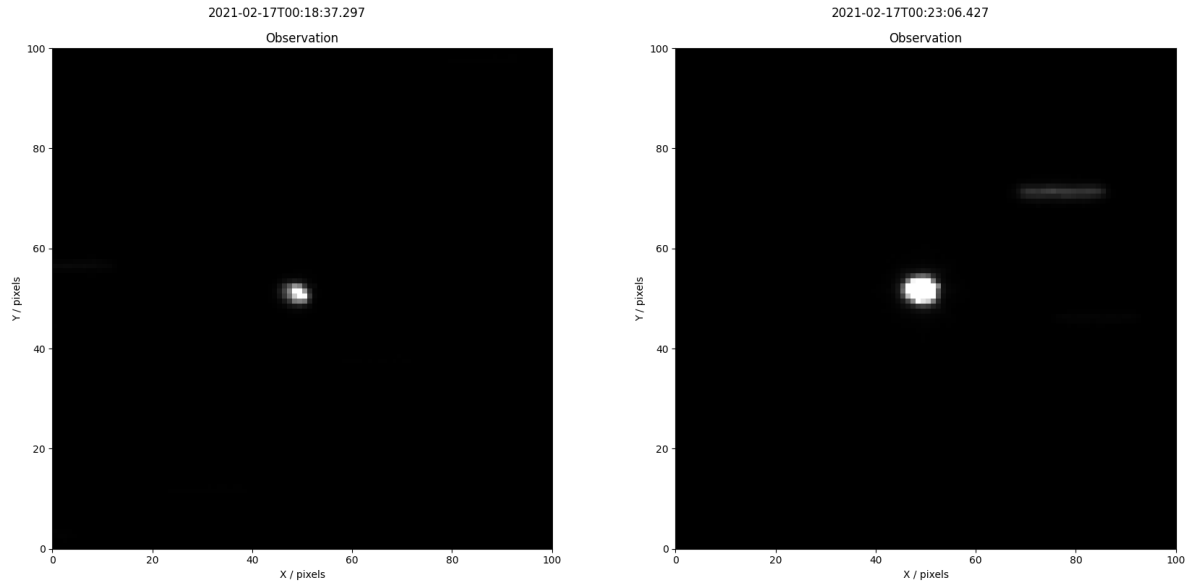

Fig. 5 – Similar to Fig. 4 except for these observations Intelsat 10-02 and MEV2 are separated such that they appear as merged sources. (left) observations showing the merged sources, appearing similar to Intelsat 10-02 alone. (right) a few minutes later a presumed 'glint' of the MEV2 source is observed.

Looking at the whole data set of observations from the Warwick Test CMOS Telescope, these glints were observed on at least ten occasions as summarized in Table 2.

Table 2 – Summary of the MEV2 Glints Observed during PHANTOM ECHOES 2

Date	**Glint Centre Time UTC**	**Window**	**Comments**
20210215	22:41:44	+/- 5 min	MEV2 and Intelsat Separable
20210216	01:27:45	+/- 5 min	MEV2 and Intelsat Separable
20210217	00:23:06	+/- 5 min	MEV2 and Intelsat Blended
20210217	00:32:47	+/- 5 min	MEV2 and Intelsat Blended
20210219	00:27:51	+/- 5 min	MEV2 and Intelsat Separable
20210219	02:49:01	+/- 5 min	MEV2 and Intelsat Separable
20210223	00:50:37	+/- 5 min	MEV2 and Intelsat Blended
20210223	01:11:43	+/- 5 min	MEV2 and Intelsat Blended
20210324	00:48:07	+/- 5 min	MEV2 and Intelsat Blended. Data not available within -5 mins.
20210324	01:10:15	+/- 5 min	MEV2 and Intelsat Blended

The properties of the telescope optics and its detector used for any observations can be expressed as a point spread function (PSF). The PSF of a sensor describes how point sources of light will appear in data collected by the sensor

and are typically similar to Gaussian functions. Even if two point sources would otherwise be individually resolvable, when two point sources are close enough together that their PSFs overlap, it can become difficult to separately identify the two contributions. The centroid of any particular observation of a source is the average pixel location of the source flux as weighted by the flux across the source's observed PSF. This typically yields a location close to the centre of the PSF for a regular PSF, where the flux is highest. In this study the Source Extractor [5] algorithm was used to estimate the flux and the centroid locations of the sources identified as Intelsat 10-02 and MEV2. In the case of blended PSFs, as is the case during some glints, the non-typical PSF results in the calculated centroid location being shifted offset in the direction of the interfering source. This characteristic of interfering sources has been used in exoplanet studies to better characterize detections [6].

As outlined above, Intelsat 10-02 is typically significantly brighter than MEV2 and to the extent that we would not expect a measurable centroid shift during typical observation conditions even when the satellites are close enough to not be separately resolved. However, during the glints this situation is changed and both sources contribute significantly and it is possible to determine the resulting centroid shift. For this study, due to the glints being short lived we can assume that the change in angular separation during a glint is negligible and it is the temporal characteristics of the glint that enhance the intensity of the flux for a short time. Fig. 6 presents an example of the observation of a glint, how its brightness varies over time, and the deviation in the centroid in units of Right Ascension (RA) and Declination (Dec) as extracted using the Source Extractor method. It is shown how as the brightness increases at the time of the glint so does the centroid shift. In the case of Fig, 6 the deviation is predominantly in the Dec direction and an absolute centroid shift offset can be determined to be 2.56 arcseconds at an angle of 54.7 degrees.

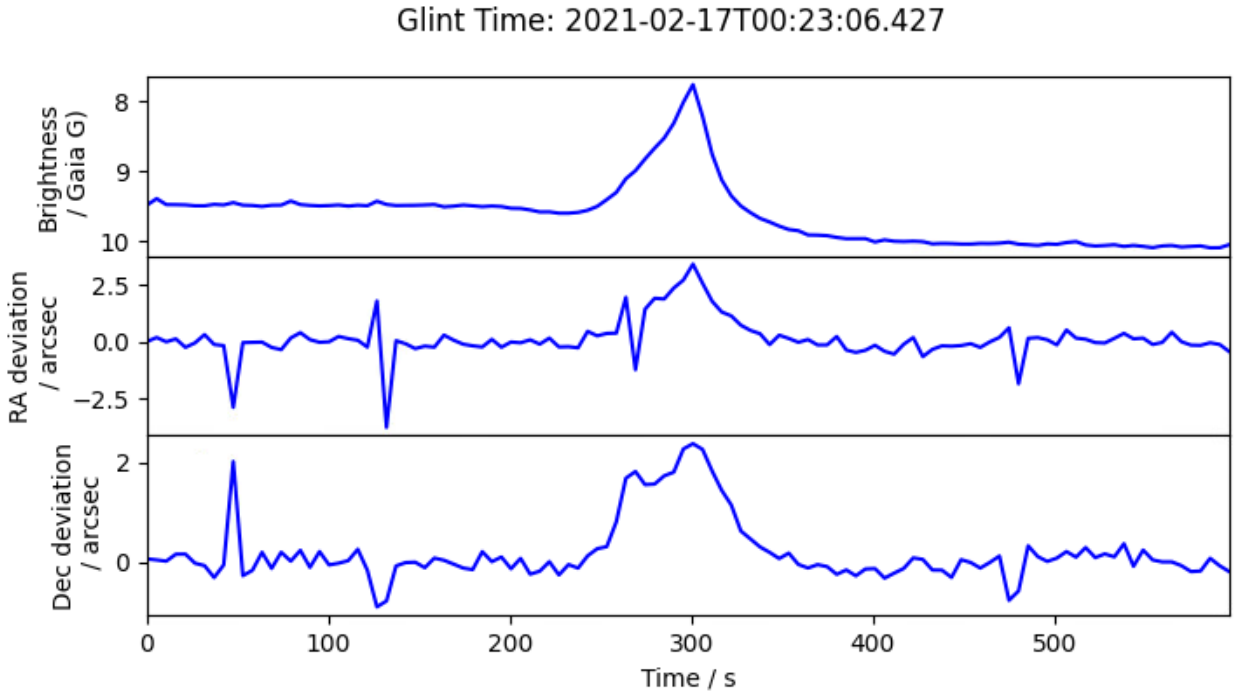

Fig. 6 – Observations of a glint observed on 17 February 2021 from a blended Intelsat 10-02 and MEV2 source. (top) brightness in Gaia G magnitude, (middle) Right Ascension (RA) deviation of the centroid shift, (bottom) Declination (Dec) deviation of the centroid shift.

4. POINT SPREAD FUNCTION MODELLING

By understanding the contribution of the two sources that cause the centroid shifts observed in the glints, it is possible to use the observed centroid shift to better understand the separation of the sources themselves. Due to the

number of observations of Intelsat 10-02 in this dataset, the PSF of Intelsat as observed with the CMOS sensor can be well estimated. It is possible to fit an idealized two dimensional PSF to the sources in the observed data. We utilise the Photutils Python library's IntegratedGaussianPRF [4] function which provides a two dimensional integrated Gaussian pixel response function which is a normalized representation of a PSF. The Source Extractor's determination of the source's flux and radius are used as input parameters. Taking the same examples as shown in Fig 4 and 5, for the separable and merged cases, the two dimensional PSF can fitted to the data to estimate the typical characteristics of the sources. This modelled fit function is shown in Fig. 6 and Fig. 7 and appears to represent the observed PSF for Intelsat 10-02 sufficiently well for this study, despite some non-symmetrical behavior not accommodated by the model.. Intelsat 10-02 also varies with solar phase angle but at least during the occasions of the observed glint the representation of Intelsat 10-02 is fairly consistent. In contrast, due to their limited number and observed variation, the glints from MEV2 are less well characterised but are typically ~2.2 - 2.6 times the peak flux intensity of Intelsat with a larger proportion of the Gaussian PSF visible above the background noise level during glints.

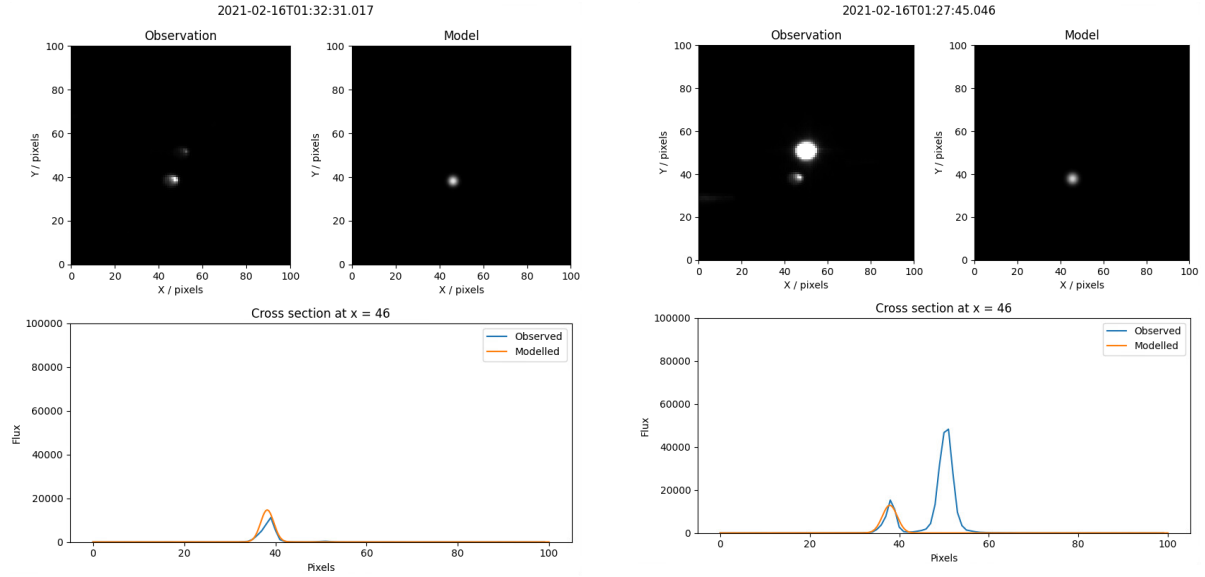

Fig. 7 –Intelsat 10-02 and MEV2 observed using the Warwick Test CMOS Telescope. (left) the 'observation' plot shows observed data from the telescope showing Intelsat 10-02 as the source brighter than MEV2. The 'model' plot is an equivalent modelled version of the same field of view including only Intelsat 10-02. The 'cross-section' plot shows the cross-sectional flux of Intelsat 10-02. (right) presented in the same format as the left group of plots, a 'glint' event for MEV2 is clearly seen.

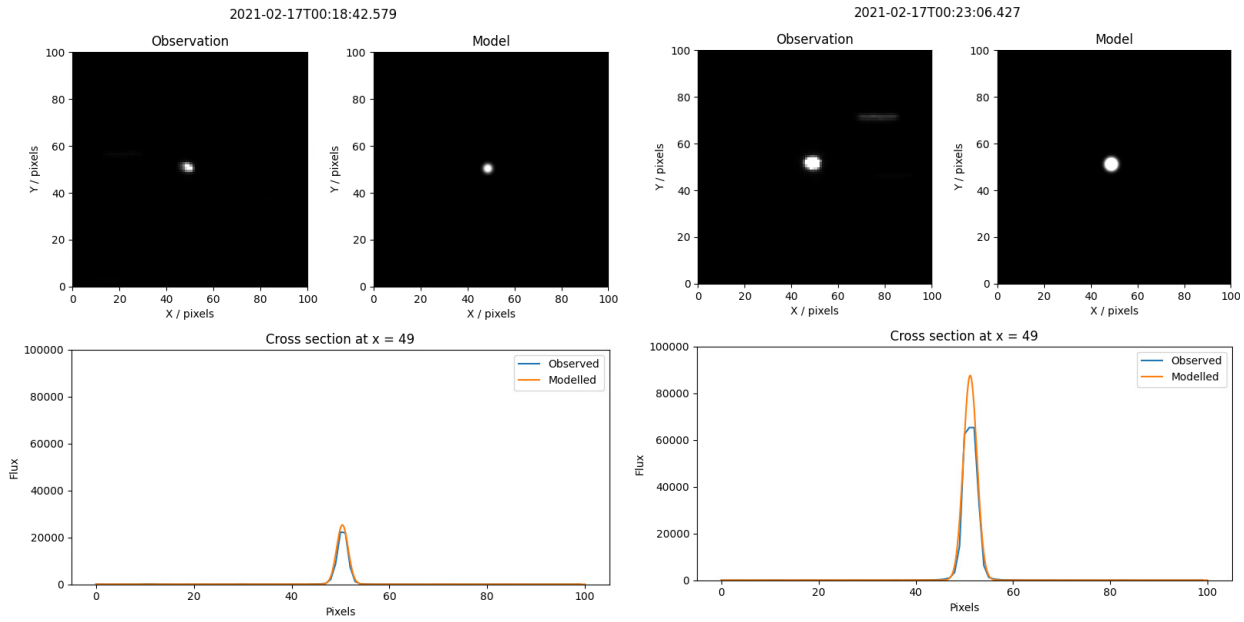

Fig. 8 - Intelsat 10-02 and MEV2 observed using the Warwick Test CMOS Telescope. (left) the 'observation' plot shows observed data from the telescope showing Intelsat 10-02 merged with MEV2. The 'model' plot is an equivalent modelled version of the same field of view. The 'cross-section' plot shows the cross-sectional flux of the merged target. (right) presented in the same format as the left group of plots, a 'glint' event is seen as part of the blended target.

Intelsat 10-02's typical total flux is typically 2.2×10^5 counts with an MEV2 glint flux being a ratio of ~2.3 to Intelsat. It is this ratio between the flux of the two sources that is a key parameter for understanding how the centroid shifts, more so than individual total fluxes. Having determined this ratio between the two objects' PSFs, a range of separations can be analysed. By representing the sources' PSFs accurately, with known pixel locations and by measuring the determined modelled centroid shift, it is possible to convert between centroid shifts and input pixel locations. In order to do so a model is established that replicates the Warwick Test CMOS Telescope data. A pixel grid frame is used with the same number of pixels horizontally and vertically as the telescope detector. Each satellite is modelled using the IntegratedGaussianPRF function with its estimated parameters and co-added into the frame at a chosen location. One satellite typically is chosen to occupy the centre of the frame, while the other is co-added at a varying pixel location so as to build up an array of potential separations. Background noise is not considered in the model due to the subtraction of the background in the original data, accepting that some variation is still present in the data. With the magnitudes of the two sources being significantly above the remaining noise, the impact of this should not be significant.

Having extracted the centroid shift and its angular direction from an observation it is possible to use this angular direction as an initial offset direction in the model. The underlying model is symmetrical around the fixed source but pixel representations, especially when coarse, can introduce asymmetries. The non-fixed source is varied with fixed spatial intervals from being separable from the fixed source, to blended, continuing until the two are directly overlapping. In this model this is represented as a source moving in the appropriate direction at a constant velocity at different time steps. For completeness, the source continues until it emerges on the opposite side of the source and is resolvable. Fig. 9 depicts four results from using the model at four different sets of source separations to replicate observations of Intelsat 10-02 and MEV2.

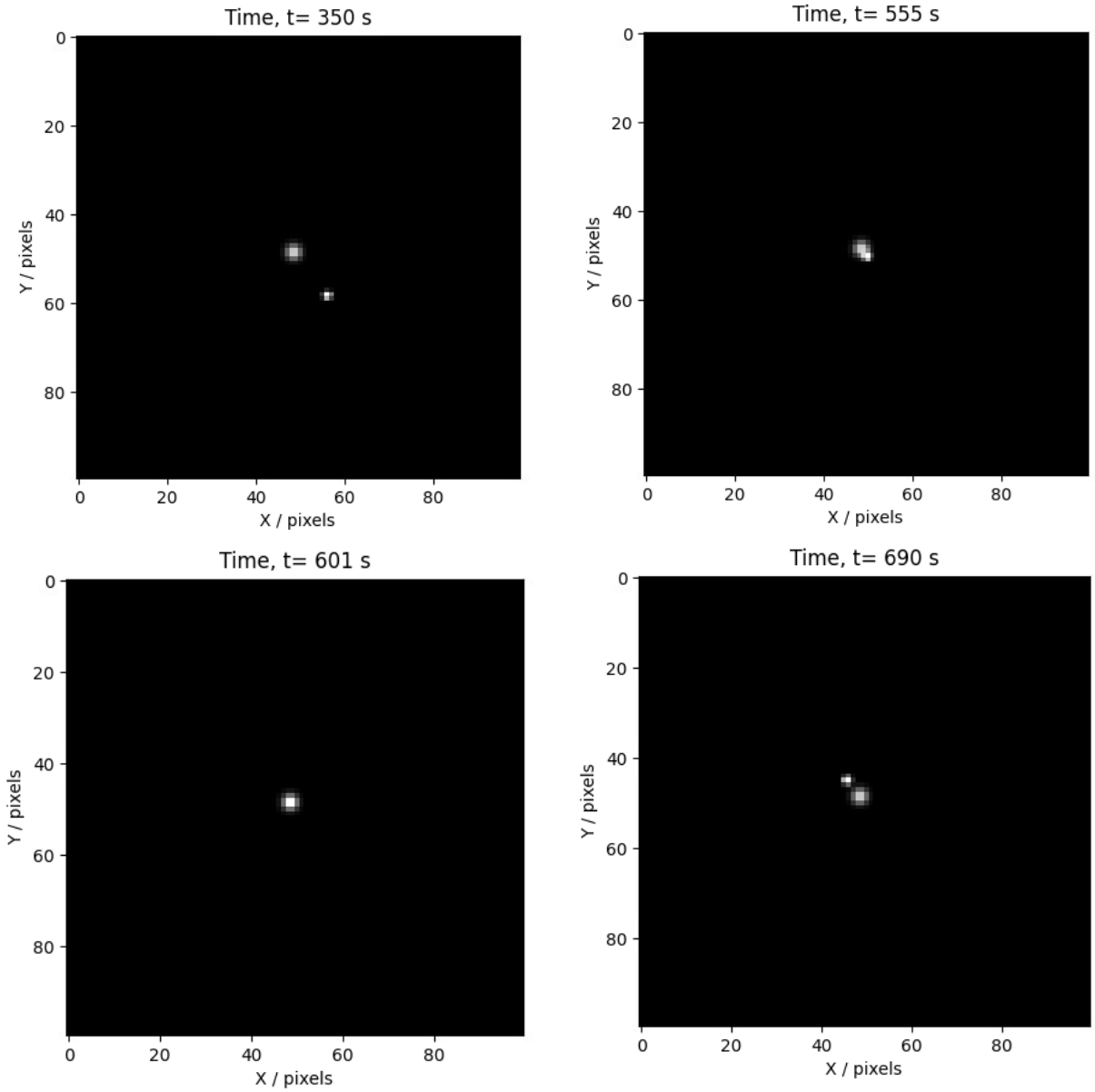

Fig. 9 – Modelled data of two sources representing MEV2 and Intelsat 10-02 at a range of separation distance on a pixel grid equivalent to that of the Warwick Test CMOS Telescope detector. (top left) – Clearly separable sources. (top right) – The two sources begin to be blended. (bottom left) – the two source directly overlapping. (bottom right) – The fainter source has passed through the brighter source and has become separable again.

An identical approach to source detection is used with this created data by using the Source Extractor algorithm to estimate the magnitude and position of the modelled satellites. The same World Coordinate System transformation is used on this data as is used on real data to yield RA and Dec coordinates that would be equivalent to that of the real data to produce relative RA and Dec separation and centroid deviation information for the two modelled satellites.

5. SEPARATION DETERMINATION

In a similar way to Fig. 6, the centroid deviation can now be plotted with respect to time in the model (which is an analogue for varying spatial separation) and is shown in Fig. 10. The figure shows that, as the two sources get closer, initially Source Extractor can still separate the two sources, resulting in zero centroid deviation, although the calculated flux does rise as sources increasingly overlap. In this example, at ~520 s a discontinuity is present which represents the point at which Source Extractor can no longer separate the two sources. This results in the largest centroid deviation offset which reduces as the two sources approach being directly overlapping. As expected, this pattern is symmetrically repeated as the moving source separates again. Using this information, it is now possible to relate the observed centroid deviation offset shift and the modelled angular separation that it would represent. For the glint observed 17 February 2021 at 00:32:47, the extracted centroid offset deviation from the Warwick Test CMOS Telescope data was observed to be 2.56 arcseconds at an angle of 54.7 degrees. Inspecting Fig. 10 and comparing this extracted deviation with the modelled deviation it is possible to relate this to the model input angular separations we would expect. In this case, this results in an estimated separation of 8.50 arcseconds.

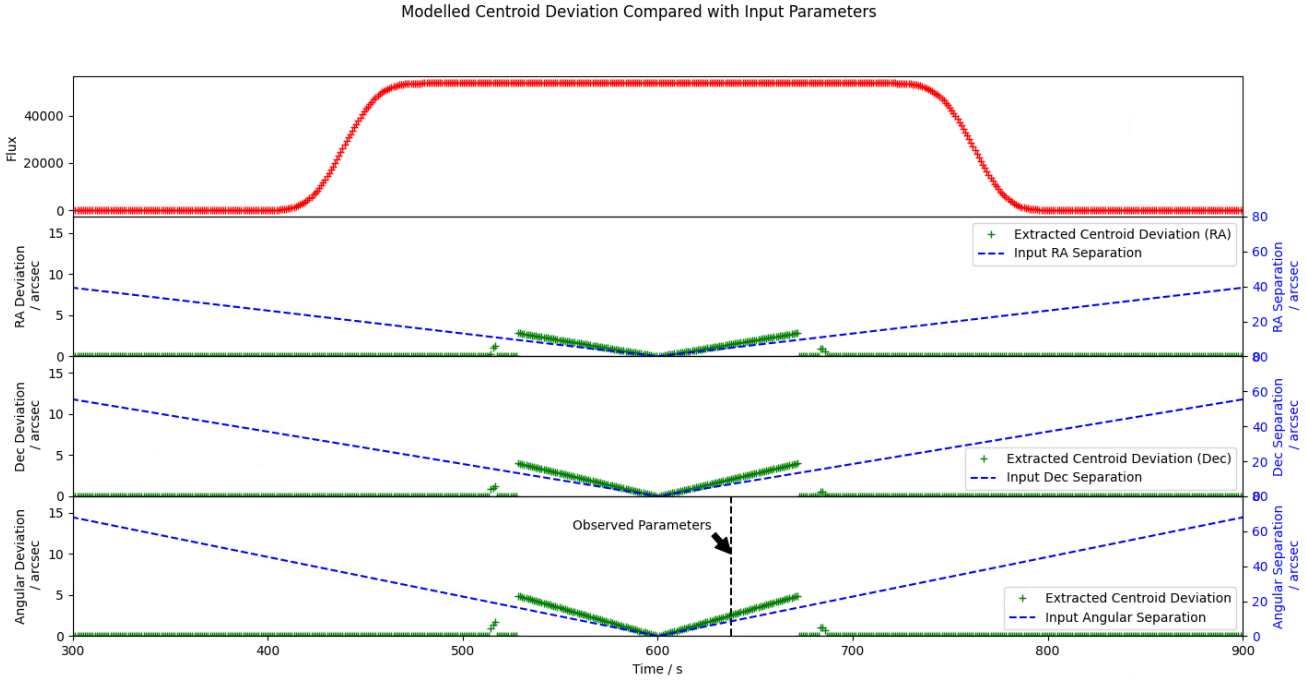

Fig. 10 – (top) – The extracted flux of the fixed source over modelled time. (upper middle) – The RA deviation with time from the model and the actual angular separation as calculated from the input parameters. (lower middle) - The declination deviation with time from the model and the actual angular separation as calculated from the input parameters. (bottom) – The overall modelled angular centroid offset deviation, the input angular separation and an indication of the parameters of the glint observed at 17 February 00:32:47.

In this case the Liverpool Telescope was observing near-simultaneously (within 41 seconds), as shown in Fig. 1 and Fig. 2 above with a resolving power that meant that the two satellites were still separable. Using an identical approach as for the Warwick Test CMOS Telescope data, utilising the Source Extractor algorithm, it is possible to determine the real separation of the two sources observed by this telescope to be 8.9 arcseconds at an angle of 51.8 degrees. Given the variability of the MEV2 glint intensity and the pixel accuracy allowed for by the Warwick Test

CMOS Telescope detector this represents a good agreement between the calculated value and this groundtruth measurement.

As a result of the variability of the MEV2 glint and the scarcity of other groundtruth data, it is important to understand the sensitivity of the model used to understand the uncertainty involved in the estimated separations it provides. In order to do this the model was run for 111 combinations of PSF flux and Gaussian width settings. The flux of the PSF was varied between -20% and 20% of the value utilised by the model (a ratio of 2.27 between Intelsat 10-02 and an MEV2 glint). The Gaussian width generally changes corresponding to the alteration in total integrated flux but it was possible to change this as well to investigate the sensitivity of this parameter. The results of sensitivity analysis are presented in Fig. 11. Here we see that changes to the primary parameter of the flux ratio appear to linearly change the calculated separation which allows for uncertainty to be adequately understood. The observed variation of the ratio between 2.2 – 2.6 reflects a ~20% variation. For the previously calculated result it would be estimated that the separation would be 8.5 ± 1.7 arcseconds. At high Gaussian width the angular separation estimated changes radically (Fig 11, top right) this is suggested to be due to the unphysicality of such high Gaussian width. The variation of the Gaussian width is generally less well characterised but observations have not presented any variations that would represent a > 100% change in this parameter and we assess its impact to be negligable.

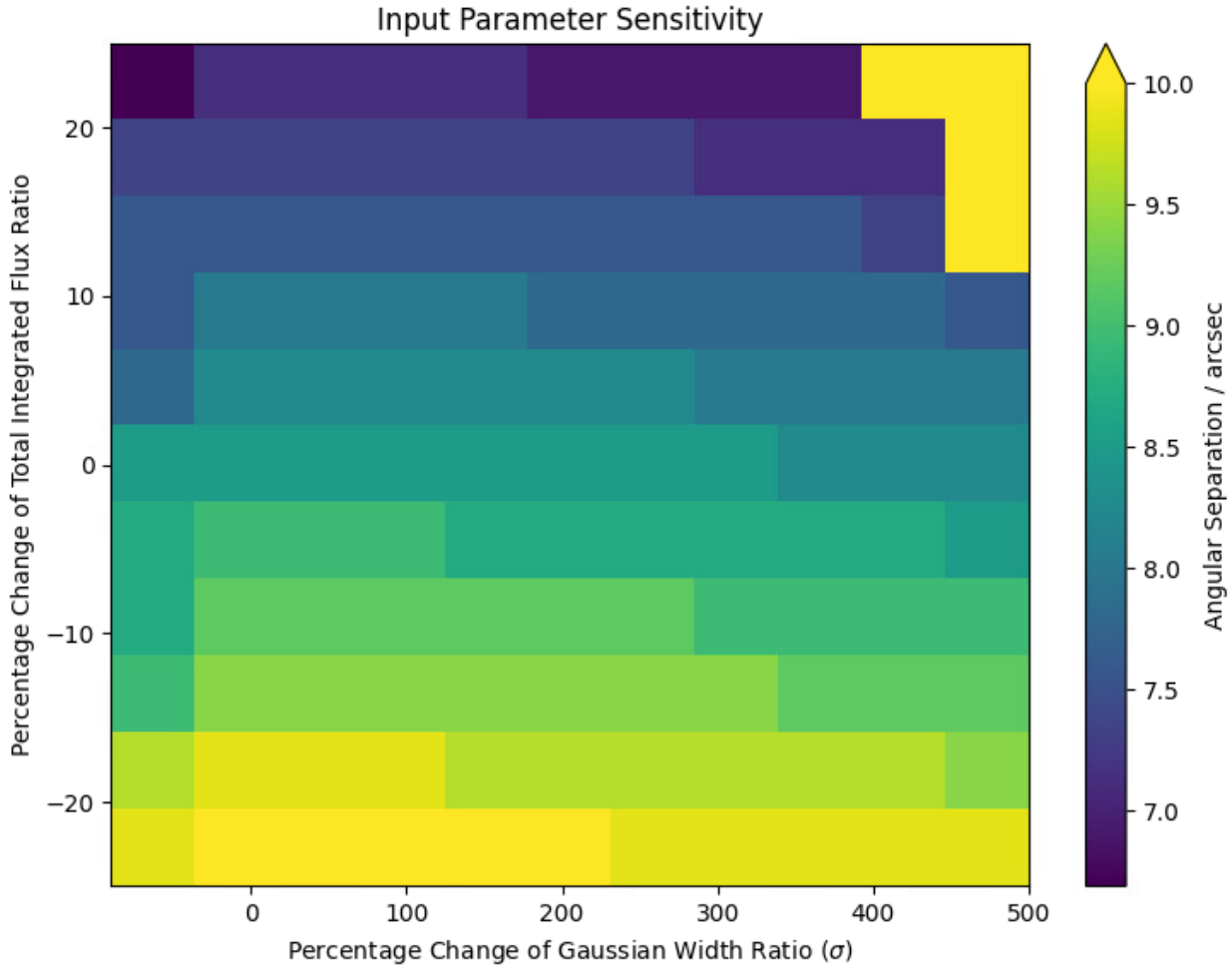

Fig. 11. – A colour map of input parameter sensitivity values for variations in the total integrated flux ratio and the Gaussian width ratio.

The centroid shift deviation offset and direction was calculated for all of the MEV2 blended with Intelsat 10-02 glints observed in the dataset. These were then compared with the centroid offsets calculated by the PSF model to determine an estimated angular separation for all of these events in the same way as described above and shown in Fig. 10. This is presented in Table 3 below.

Table 3 – Summary of the Results for Glints Observed During the PHANTOM ECHOES 2 Experiment

Date	**Glint Centre Time (UTC)**	**Observed Centroid Deviation Direction (degrees)**	**Observed Centroid Deviation Offset (arcsec)**	**Extracted Separation from Modelled PSF (arcsec)**
20210217	00:23:06	34.9	4.149	13.73 ± 2.75
20210217	00:32:47	54.7	2.562	8.50 ± 1.70
20210223	00:50:37	-130.3	2.809	9.18 ± 1.84
20210223	01:11:43	-110.3	2.540	8.49 ± 1.70
20210324	00:48:07	-96.1	2.380	7.81 ± 1.56
20210324	01:10:15	-109.3	1.879	6.23 ± 1.25

6. DISCUSSION

It has been demonstrated that angular separations with a well characterised uncertainty can be determined from telescope observation data where the objects of interest were not individually separable. Examples were provided using glints observed from MEV2 during its rendezvous and proximity operations with Intelsat 10-02. In this case the glints allowed for this approach to work successfully. However, this approach can potentially be utilised for any similar scenario where the two merged sources have previously been well characterised and where one is not so significantly brighter than the other that any centroid shift is not detectable. Fainter objects will still have some influence on the centroid shift of bright objects but the sensor performance required to detect the change will be more significant for a larger difference.

The ability to individually resolve targets that are closely spaced is dependent on the resolving power of the telescope. To be able to continue to detect and track closely spaced objects requires increasing levels of sensor performance the closer the objects become, potential requiring the use of more costly systems. This technique provides a way in which to continue to detect and track objects using lesser performance systems. As rendezvous and proximity operations, similar to that of Intelsat 10-02 and MEV2 become increasingly common the techniques covered in this paper should help inform performance requirements for future SDA sensing capabilities.

7. REFERENCES

[1] S George, A Agathanggelou, G Privett, P Halpin, W Feline, A Ash, P Chote, L Scott, J Skuljan, J Alvino, J Frith, PHANTOM ECHOES 2: A Five-Eyes SDA Experiment on GEO Proximity Operations*, Proceedings of AMOS Conference*, 2021

[2] C Meredith, G Privett, S George, P Halpin, W Feline, Novel Image Alignment Technique for Extraction of Astrometry and Photometry from Small Field of View Astronomical Sensors, *Proceedings of AMOS Conference*, 2022

[3] P Chote et al, High-precision light curves of Geosynchronous objects I: The PHANTOM ECHOES 2 campaign, in preparation, 2023
[4] L Bradley., astropy/photutils: 1.8.0 (1.8.0). *Zenodo*. https://doi.org/10.5281/zenodo.7946442, 2023
[5] E Berton, S Arnouts, S., SExtractor: Software for source extraction, *Astronomy & Astrophysics Supplement 317*, 393, 1996
[6] M Günther et al, Centroid vetting of transiting planet candidates from the Next Generation Transit Survey, *Monthly Notices of the Royal Astronomical Society,* 472, 2017